Conf-930159--54

LBL-33786
UC-~~109~~ 404

Center for Advanced Materials

CAM

Presented at Biomedical Optics, Los Angeles, CA,
January 16–23, 1993, and to be published in the Proceedings

Quantitative Analysis of Scanning Tunneling Microscopy Images for Surface Structure Determination: Sulfur on Re(0001)

D. F. Ogletree, P. Sautet, J. C. Dunphy, and M. B. Salmeron

February 1993

RECEIVED
AUG 20 1993
OSTI

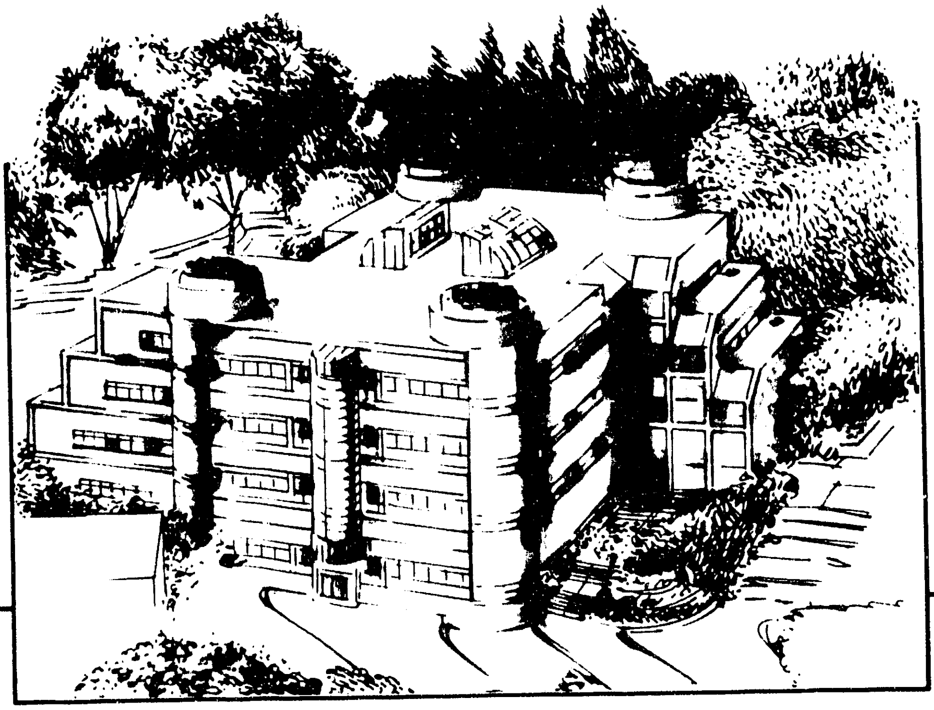

Materials and Chemical Sciences Division

Lawrence Berkeley Laboratory • University of California

ONE CYCLOTRON ROAD, BERKELEY, CA 94720 • (415) 486-4755

Prepared for the U.S. Department of Energy under Contract DE-AC03-76SF00098

[illegible]

DISCLAIMER

This document was prepared as an account of work sponsored by the United States Government. Neither the United States Government nor any agency thereof, nor The Regents of the University of California, nor any of their employees, makes any warranty, express or implied, or assumes any legal liability or responsibility for the accuracy, completeness, or usefulness of any information, apparatus, product, or process disclosed, or represents that its use would not infringe privately owned rights. Reference herein to any specific commercial product, process, or service by its trade name, trademark, manufacturer, or otherwise, does not necessarily constitute or imply its endorsement, recommendation, or favoring by the United States Government or any agency thereof, or The Regents of the University of California. The views and opinions of authors expressed herein do not necessarily state or reflect those of the United States Government or any agency thereof or The Regents of the University of California and shall not be used for advertising or product endorsement purposes.

Lawrence Berkeley Laboratory is an equal opportunity employer.

This publication has been reproduced from the best available copy

LBL-33786
UC code 109

QUANTITATIVE ANALYSIS OF SCANNING TUNNELING MICROSCOPY IMAGES FOR SURFACE STRUCTURE DETERMINATION:
SULFUR ON Re(0001)

D.F. Ogletree, P. Sautet[1], J.C. Dunphy, and M.B. Salmeron

Materials Sciences Division
Center for Advanced Materials
Lawrence Berkeley Laboratory
University of California
Berkeley, CA 94720 U.S.A.
and
Department of Physics
University of California
Berkeley, CA 94720 U.S.A.

[1] Laboratorie de Chemie Theoretique, ENS Lyon, France; Institut de Recherche sur la Catalyse, Villeurbanne, France

---

ACKNOWLEDGMENT
This work was supported by the Director, Office of Energy Research, Office of Basic Energy Sciences, Material Sciences Division, U.S. Department of Energy under contract No. DE-AC03-76SF00098.

Quantitative analysis of Scanning Tunneling Microscopy images for surface structure determination: Sulfur on Re(0001)

D. Frank Ogletree, Philippe Sautet[1],
James C. Dunphy[2] and Miquel Salmeron

Material Sciences Division, Lawrence Berkeley
Laboratory, Berkeley CA 94720

1) Laboratorie de Chemie Theoretique, ENS Lyon,
France and Institut de Recherche sur la Catalyse, Villeurbanne, France

2) and Department of Physics, University
of California, Berkeley CA 94720

ABSTRACT

Scanning Tunneling Microscopy (STM) images of adsorbed atoms and molecules on single crystal substrates provide important information on surface structure and order. In many cases images are interpreted qualitatively based on other information on the system.

To obtain quantitative information a theoretical analysis of the STM image is required. A new method of calculating STM images is presented that includes a full description of the STM tip and surface structure.

This method is applied to experimental STM images of sulfur adsorbed on Re(0001). The effects of adsorption site, adsorbate geometry, tip composition and tunnel gap resistance on STM image contrast are analyzed. The chemical identity of the tip apex atom and the substrate subsurface structure are both shown to significantly affect STM image contrast.

1. INTERPRETATION OF STM IMAGES

Scanning Tunneling Microscopy (STM) is a powerful tool for the atomic-scale study of surface structure. Over the last decade STM images of hundreds of metal and semiconductor surfaces have been reported with atomic-scale resolution.[1,2] From the beginning, the interpretation of these images has posed problems.

STM images depend on both the geometrical and electronic structure of the tunneling tip and the surface being imaged. Even though STM images resolve atomic scale features and show the surface unit cell, there may be no simple correspondence between the number of atoms on the surface and the number of bright spots or protrusions in the image. STM images of the basal plane of graphite provided an early example of this problem. Although there are two atoms in the surface unit cell, STM images usually show only one maxima.[2]

The full power of STM will only be realized when theoretical tools are developed that can relate STM image contrast to surface structure and chemistry. Unfortunately a full theoretical description of the tunneling process is an exceedingly difficult problem. The electronic structure of the tip and surface interact.

Surface relaxations and reconstructions have strong effects on STM images and must be included. In most real experiments, the detailed structure of the tunneling tip is uncertain.

To simulate an STM image, the tunnel current must be calculated for several different tip-surface positions. A large number of nonequivalent atoms are included in the description of the tip-surface region, and there is no symmetry either perpendicular or parallel to the surface to simplify calculations. Therefore any attempt to analyze experimental STM images will involve various types of approximations.

STM theory has been considered by many authors. Tersoff and Hamann[3] analyzed tunneling in the limit of weak coupling between tip and surface (Bardeen approximation). In this limit they showed that a constant current STM image at small bias voltage was equivalent to a surface of constant local density of states at the Fermi energy, and that any spherically symmetrical tip would give the same image as a "delta function" tip. Lang[4] analyzed the effects of chemisorption. electronic structure and strong tip-surface interaction in detail by treating the bulk surface and tip in the jellium model, where most atoms are replaced by a uniform electron density.

These approaches provided key insights into the general nature of STM imaging, however they do not allow detailed analysis of STM experiments. There is experimental evidence that the chemical identity of the tip atom can directly effect STM images,[5,6] and this is not addressed in Tersoff's theory. Likewise, Lang's jellium approximation has removed the details of surface structure.

Ciraci, Baratoff and Batra *et al.*[7] have taken a different approach and treated the problem of currents and forces between tip and surface rather exactly with *ab initio* self consistent pseudopotential calculations. They apply this method to a simple system, with both tip and surface represented by bulk terminated Al(001) slabs. Cyclic boundary conditions were used with a cell of only one Al atom per layer. Description of this relatively simple system required ~ 500 plane waves and massive calculations. For the foreseeable future this type of calculation will be restricted to detailed analysis of simple model systems. Analysis of experimental systems with many inequivalent atoms must use approximate methods that are more computationally efficient.

2. STM THEORY: A SCATTERING APPROACH

In this work we describe STM electron tunneling as a scattering process. The bulk states of the tip material are coupled to the bulk states of the surface through a "tip-adsorbate-surface" (TAS) region. The TAS region includes any atoms or molecules chemisorbed on the surface, any relaxed or reconstructed layers of the substrate, and the last atomic layers of the tip. On each side of the TAS region are semi-infinite solids corresponding to the tip wire and to the substrate.

The calculations follow a quantum chemistry approach developed by Sautet and Joachim,[8] using atomic-like orbitals centered on the different atoms. This real-space representation has important advantages when it comes to understanding the results of calculations in physical terms, as discussed below. The electronic states of this system are expressed in terms of the Hamiltonian matrix elements $\mathbf{H}_{ij}$. A scattering matrix **S** is calculated from **H**. It is possible to make a formal transformation of **S** to eliminate states in the TAS region from the solution, so the new scattering matrix couples bulk tip states to bulk surface states. The tunnel current or conductance can then be calculated from the **S** matrix.

This idea can be understood by thinking about the basic quantum mechanics problem of one dimensional tunneling through a barrier. The final result is the amplitude and phase of reflected and transmitted waves. This answer has the same form for a simple square barrier or a complex one with multiple heights -- outside of the barrier region the tunneling is described by the reflected and transmitted waves, only the amplitude and phase depend on the details of the barrier. In the same way, the numerical values of the energy-dependent S matrix elements depend on the details of the TAS region but the bulk states of the tip and substrate do not.

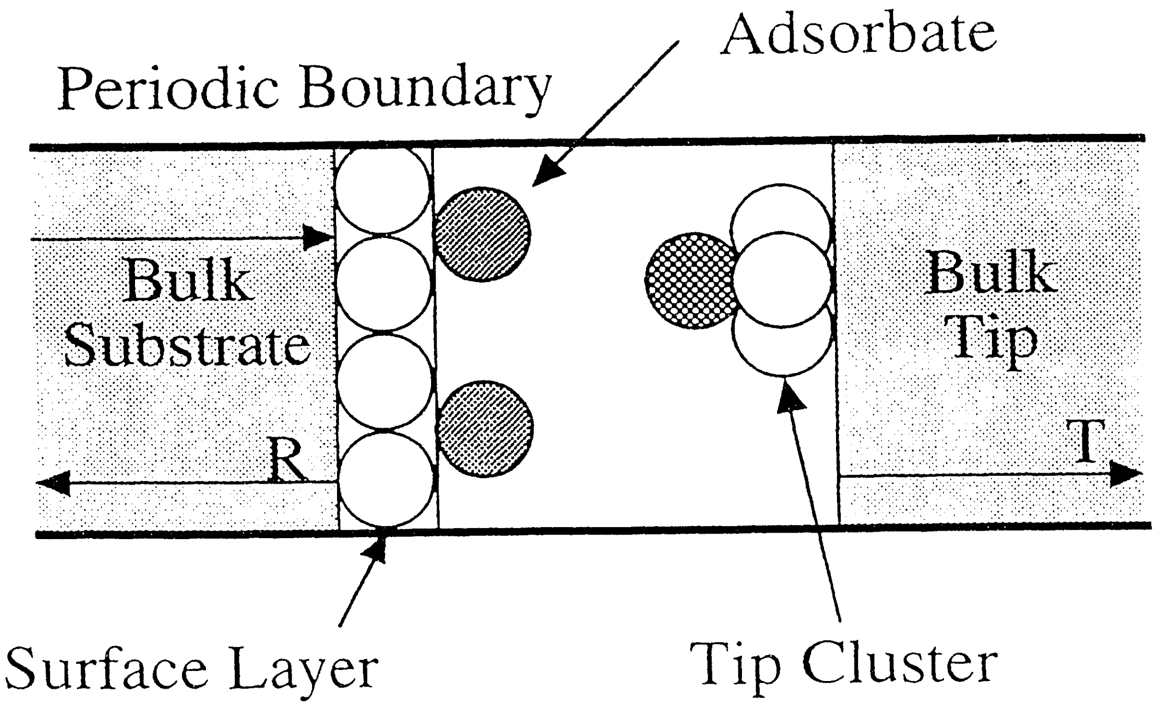

Figure 1. The basic description of the tunneling process. Electron waves travelling through the bulk substrate (left) encounter the Tip-Adsorbate-Surface region. These waves are backscattered or transmitted into the bulk tip wire. The relative amplitudes and phases are described by the scattering matrix S. For tip to surface tunneling (positive sample bias) the directions are reversed.

This method of describing tunneling is exact -- the approximations come in when the $\mathbf{H}_{ij}$ matrix elements are calculated. This is done using the extended Hückel molecular orbital approximation, where the off diagonal matrix elements are approximated as the product of the overlap of the orbitals i and j with the sum of their energies. This approximation has been shown to give a good qualitative description of the wave functions of adsorbates on metal surfaces.[9] For the STM calculations there are no adjustable Hückel parameters and the overlap integrals are calculated exactly.[5,8]

The STM calculations are all done in the limit of small bias voltages. This is a good assumption for most STM experiments on metal surfaces. To simulate an image in the constant height mode, the tunnel current is calculated with the tip at a number of different points within the surface unit cell. For constant current images, at each point the current is calculated for different heights and the z value for the desired current is determined by interpolation.

3. (2X2) SULFUR ON RE(0001)

The rhenium calculations used four 2x2 unit cells, or 16 metal atoms per layer with cyclic boundary conditions. Bulk values were used for the Re lattice. The tip was represented by a four atom tetrahedron on a metal surface. STM images were simulated by calculating tunnel current or tip height at 35 nonequivalent points within the 2x2 unit cell. Topographic images were calculated at a tunnel gap resistance of 30 to 60 megohms, and current images at gap widths of 3 to 6 angstroms.

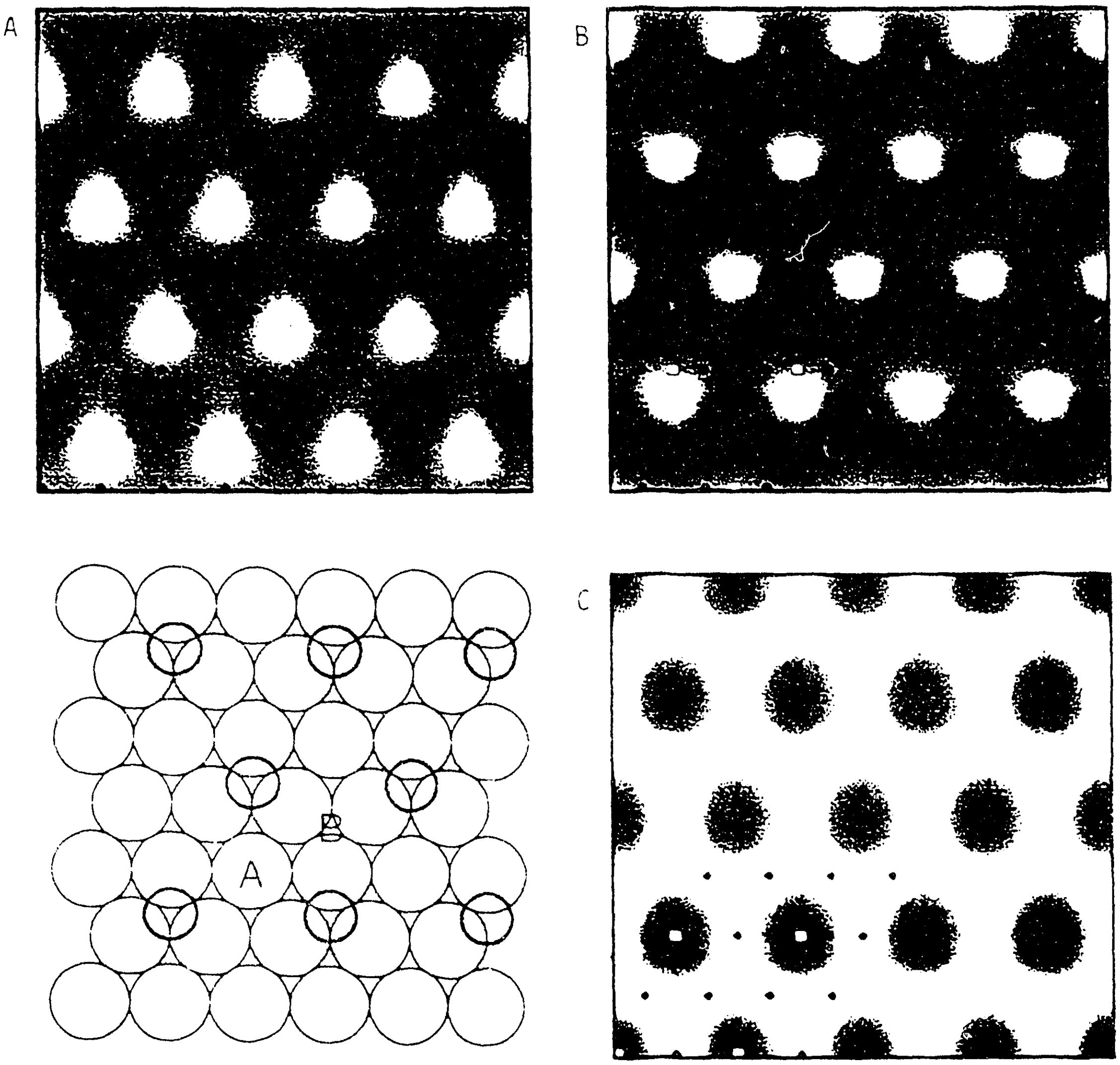

Figure 2. Topographic STM images calculated for sulfur adsorbed in A) 3-fold hollow sites, the LEED result (top left), in B) bridge sites (top right), in C) top sites (bottom right), and a schematic of the LEED geometry (bottom left). The small squares in the STM images indicate the S atom positions and the dots represent Re atoms. In the schematic the shaded circle is the S ionic radius and the smaller circle the covalent radius. The A and B sites are discussed in section 3 and figure 4.

Sulfur chemisorption on transition metal surfaces at low coverages has been widely studied by structure sensitive methods, including Low Energy Electron Diffraction (LEED), photoelectron diffraction, ion scattering and extended x-ray absorption fine structure (SEXAFS and EXAFS).[10] LEED structure calculations show that sulfur adsorbs in the 3-fold HCP hollow sites 1.67 angstroms above the Re(0001) surface layer to form a (2x2) lattice.[11] On the close packed (0001) surface of HCP (hexagonal close-packed) metals and the (111) surface of FCC (face-centered cubic) metals there are two types of three fold hollow sites. The HCP hollow has a second layer atom centered under the site and the FCC hollow does not.

A theoretical simulation of the STM image was calculated for (2x2) sulfur on Re(0001) using the known LEED geometry. As a check, STM images were also calculated for sulfur adsorbed in bridge and on-top sites with the same S-Re bond lengths. The results are shown in Figure 2.

Figure 2 shows that the bright maxima in the STM images correspond to the location of the S atoms only for hollow site adsorption. For the bridge sites the maxima is shifted off the S position, and for top sites the S atoms are minimums in the STM images.

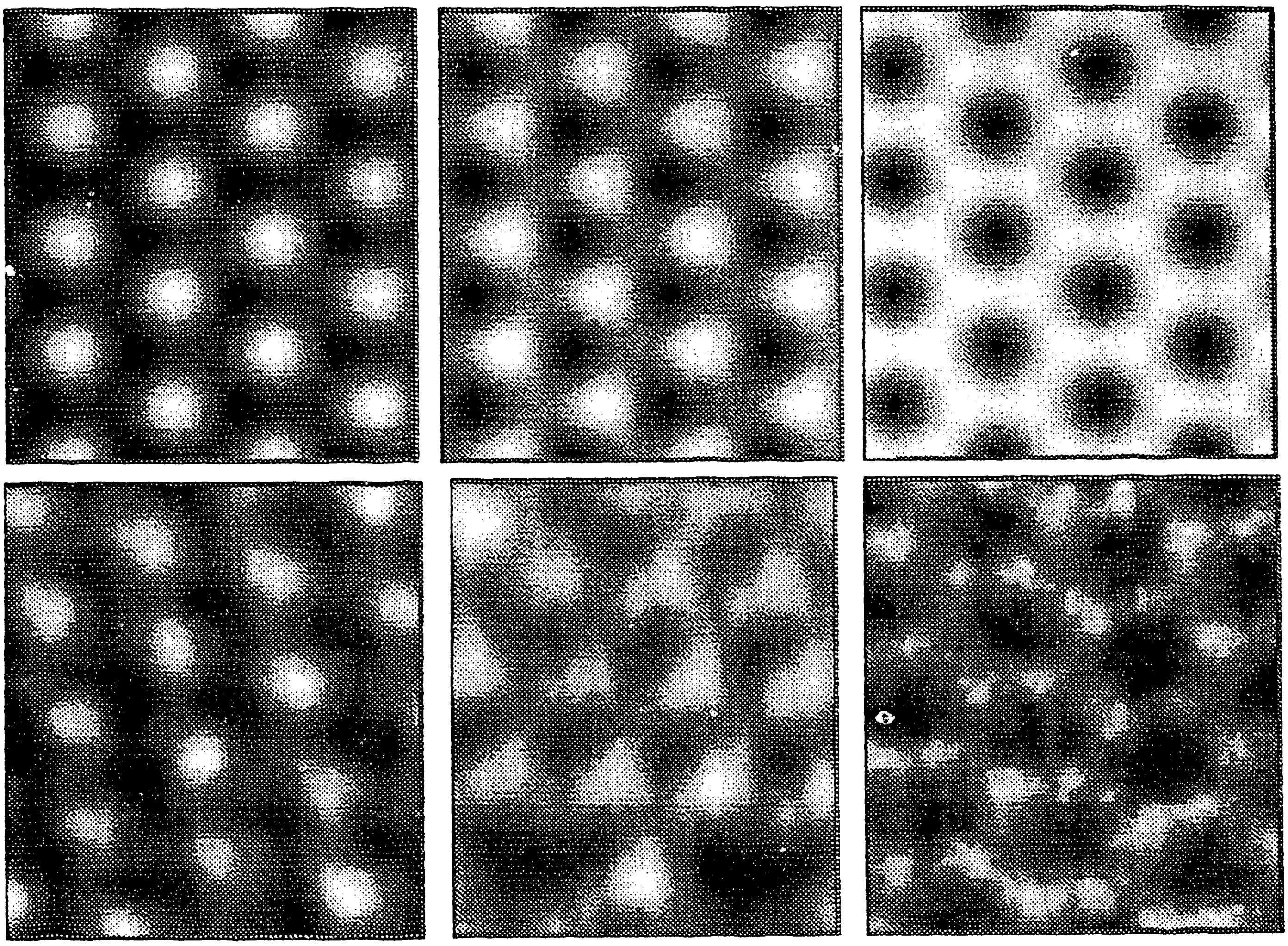

Figure 3. Comparison of theoretical simulations for different tips (top) with experimental STM images (bottom). Images with round maxima (left) correspond to S (or C) atom tips, images with triangular maxima correspond to metal atom tips (center) and honeycomb images correspond to blunt two and three atom tips (right).

4. TIP EFFECTS ON STM IMAGES

The experimental STM images of (2x2) S on Re(0001) were not completely reproducible. Three general types of STM image contrast were found: some with round maxima on a (2x2) lattice, some with triangular maxima, and some with 'Y' shaped maxima where the Y's overlapped to form a 'honeycomb' hexagonal mesh.[5] Sometimes one type of image contrast would spontaneously switch to another type. Observations of point defects and domain boundaries ruled out multiple-tip effects.

Theoretical STM calculations were used to investigate the effect of changes in tip structure on image contrast (Figure 3). The tip was modeled by a four atom tetrahedron. Since Pt/Rh alloy tip wires were used, images were calculated for tips terminating in Pt, Rh and Re transition metal atoms. Images were also calculated for tips terminating in S and C atoms since S adsorbs readily on Pt, and carbon is a common contaminant in UHV studies of metals. Finally, images were calculated for blunt tips consisting of two and three atom clusters of metal atoms instead of a four-atom tetrahedron.

Calculations showed that the variation in experimental STM images could be explained by changes in tip structure. Since the STM calculations use a real-space basis, it is possible to "dissect" the theoretical results and interpret them in physical terms.

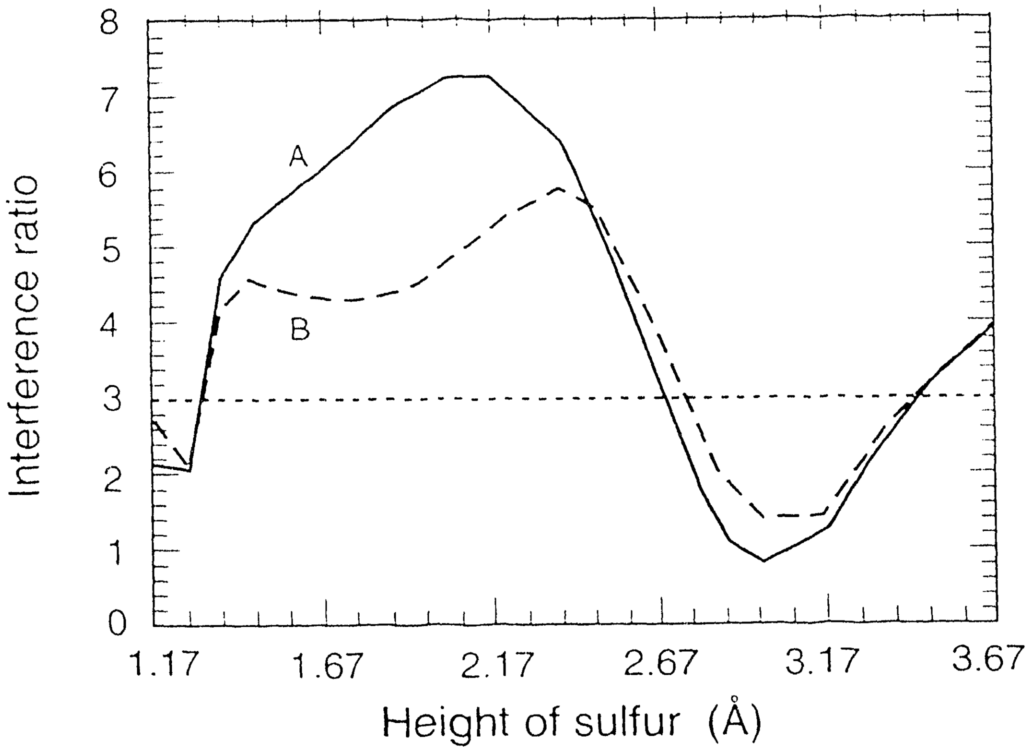

Figure 4. Calculated tunnel current as a function of sulfur-rhenium separation for a Pt tip equidistant from three S atoms. The horizontal line shows the sum of tunneling current intensity from the three S atoms (no interference). The solid and dashed lines show the sum of tunneling *amplitudes* from the S atoms (with interference) with the tip in an **A** site (solid) or **B** site (dashed) (see text). Interference effect produce large changes in tunnel current in some cases.

The main channel for the tunnel current was through the *s*-states of the tip apex atom(s) through the chemisorbed S atoms. "Direct" tunneling from the tip to the atoms of the Re surface was negligible in comparison. Tunneling from tips with an electronically "small" apex atom like S or C was primarily through the closest surface S atom. This produced round maxima and a relatively large image corrugation. The wavefunction of tips ending in an electronically larger metal atom (Pt, Rh, Re) overlapped with more than one S atom, producing triangular maxima and reduced corrugation.

Images with blunt two and three atom tips depend on the orientation of the tip trimer relative to the substrate lattice. When the tip is positioned directly over a sulfur atom in a hollow site, the three tip atoms can be aligned with the substrate atoms (eclipsed geometry) or rotated by up to 60 degrees (staggered geometry). The blunt tip has the largest overlap with the S atoms and produces images with the smallest corrugation. In the eclipsed orientation the blunt tip produces honeycomb images, as shown in Figure 3. In the staggered orientation, the images have triangular maxima similar to those produced by a single metal atom but with reduced corrugation.

Images were also calculated with intermediate trimer orientations. As the trimer is rotated from the eclipsed to the staggered geometry, the honeycomb images gradually become more asymmetrical, appearing as linked zig-zag chains, which then transform into broad triangular maxima as the rotation reaches the staggered geometry. A few calculations were also done for dimer tips with two Pt atoms. The resulting images were generally similar but less symmetric to those of trimer tips. The images also depended on the relavtive orientation of the dimer. Many orientations gave asymmetric honeycomb images with more intensity along one direction, resulting in a zig-zag appearence. Asymmetrical zig-zag chain images were observed experimentally

A closer examination of the calculated images for a single metal atom tip (Figure 3, left side) reveals another important effect. In this image the triangular maxima correspond to the S atom positions. When the tunneling tip is equidistant from three S atoms, the main contributions to the tunnel current are through these neighboring S atoms. Tunneling from the metal surface to the tip apex, or from the S atoms to the tip shaft is negligible in comparison. There are two different types of sites between three S atoms. The **A** sites are where the points of the triangular maxima come together, and the **B** sites are those surrounded by the sides of the triangles. In the schematic of Figure 2, the A sites are above a Re atom that is not in contact with S atoms, and the B sites are above triangles of Re atoms.

The tunnel current at both **A** and **B** sites is due to the overlap of the tip *s*-state with the *s*-states of three equidistant S atoms. However the calculcted currents are different -- the **A** sites are brighter than the **B** sites, giving a triangular appearance to the image maxima. This is due to quantum interference when the tunneling amplitudes through the three S atoms are summed. The magnitude of the contribution from each S atom is the same in **A** and **B** sites, but the relative phases are different, leading to constructive interference at the **A** sites and destructive interference at the **B** sites.

This interpretation shows the value of a calculation using a real-space basis set. It is relatively easy to "turn off" the interference term and see how this effects the image. Figure 4 shows the interference contributions at **A** and **B** sites for a variety of S adsorption geometries. The horizontal dashed line at amplitude 3 is the tunnel current with no interference (three times the single channel current). In this case **A** and **B** sites are equivalent. The solid (A site) and broken (B site) lines show the tunnel current with interference. The size of the interference effect varies as the spacing between the S atoms and the Re surface is varied. For a S-Re spacing of 1.67 angstroms (the LEED geometry) there is a significant enhancement of **A** sites relative to **B** sites.

It is important to stress that this interpretation is based on the results of calculations. Interference effects are only one factor which can influence image contrast. In the case of (2x2) S on Re(0001) with a metal tip, interference has a major effect on image contrast. For an S atom tip, interference effects are much smaller, since the smaller tip wavefunction usually overlaps with only one S atom at a time. In case of S on Mo described below, interference effects are relatively small and geometrical effects dominate.

5. C(2X2) SULFUR ON MO(001): STRUCTURE EFFECTS

Experimental STM studies[12] and theoretical STM calculations[13] have been made for the c(2x2) sulfur overlayer on Mo(001). Sulfur chemisorbes in 4-fold hollow sites on Mo(001). Since the (001) surfaces of bcc metals are relatively open, there is also a strong interaction between the chemisorbed S atoms and the second-layer Mo atoms, located directly below the center of the 4-fold hollow site.

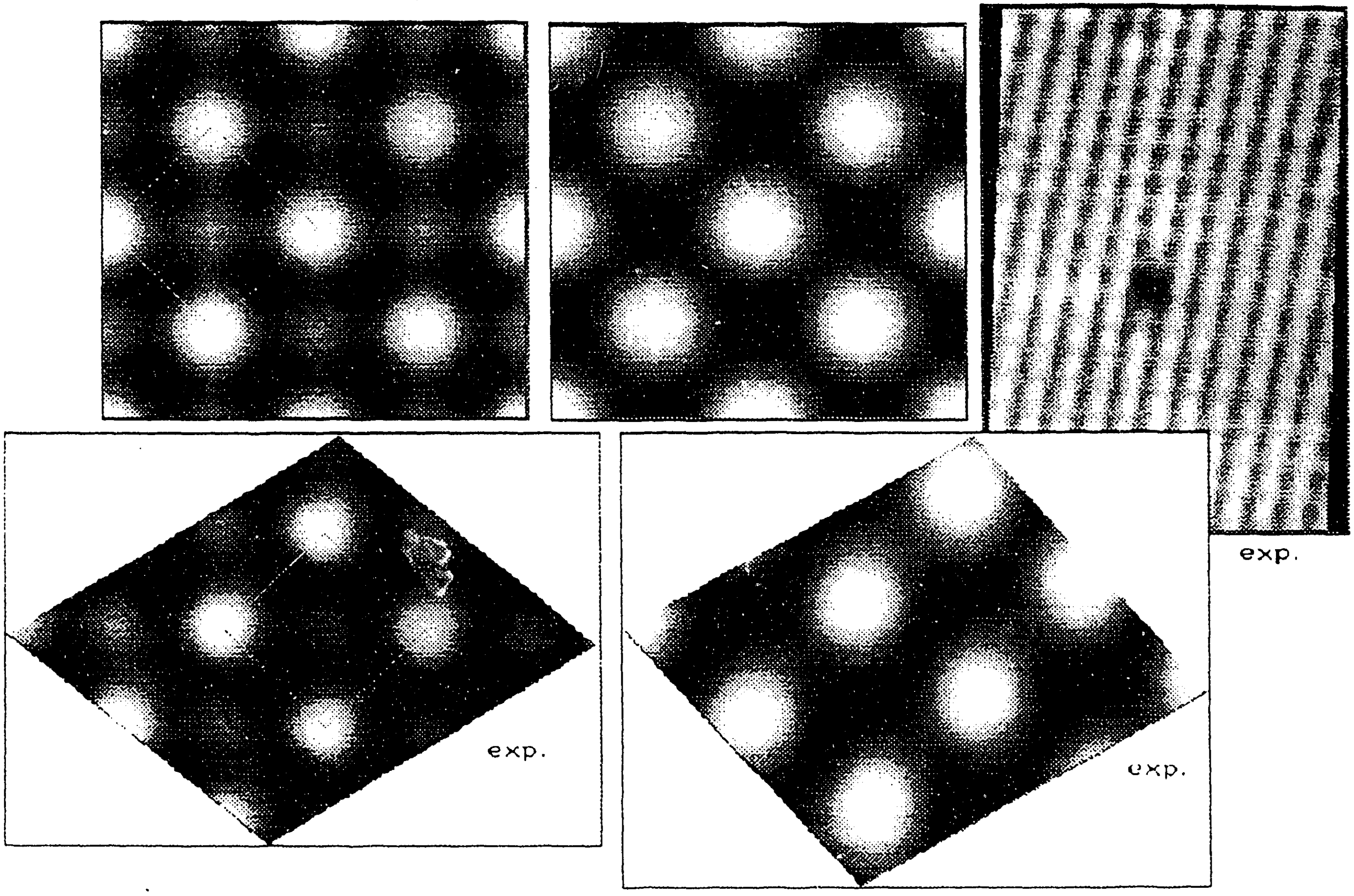

Calculated and experimental images of c(2x2) S on Mo(100)

Figure 5. Experimental and theoretical images for the c(2x2) S overlayer on Mo(001). The image at right is a relatively large experimental image showing a point defect. At left are averaged unit cells from two types of experimental images (below), and the corresponding theoretical calculations (above).

Two general types of experimental STM images were observed. In one case there is on bright maxima per unit cell, in the other a weak secondary maxima can also be observed, as shown in Figure 5.

Theoretical STM calculations were made using the bulk geometry for the molybdenum surface and a S-Mo bond length corresponding to the sum of the covalent radii with S adsorbed in 4-fold hollow sites. Low coverage S adsorption structures have been determined for several surfaces, and in all cases S adsorbed in the highest coordination site available with a sulfur-metal bond length within ~ 0.15 angstroms of the sum of the covalent radii.[10]

As in the case of S on Re(0001), the two types of images were associated with chemically different tips. The images with a single maxima correspond to metal tips. The image contrast is dominated by tunneling through the S atoms (Figure 5 right side). An S atom tip with a smaller electronic radius can fit between the adsorbed S atoms to some extent and there is a small direct tunneling contribution from the Mo atoms. This produces the weak secondary maxima observed in some images (Figure 5 center).

Further calculations were made to explore the possibility of using STM to determine the geometry of the surface in addition to the adsorption site. In LEED structure calculations, for example, theoretical I-V curves for diffracted beams are calculated for a given structural model with different values of geometrical parameters such as bond lengths and surface layer relaxations. Sometimes LEED calculations must be carried out for several different models. These calculations are compared to the experimental results, and the best match gives the preferred surface structure. This same method has been applied to STM image data.

In the case of c(2x2) S on Mo(001) there are two main geometrical parameters in the 4-fold adsorption site model, the vertical separation between the S atoms and the first Mo layer, and the vertical displacement of the second layer Mo atom directly below the S adsorption site, or second layer buckling. STM images were calculated assuming a metal tip and a c(2x2) overlayer of S atoms adsorbed in 4-fold hollow sites. The S-Mo distance ranged from 0.90 to 1.10 angstroms and the second layer bucking from 0.00 to 0.25 angstroms in 0.05 angstrom increments. Positive buckling reduces the distance between the second layer Mo atom and the S atom. The results are shown below in Figure 6.

STM image contrast is significantly affected by changes in the atomic positions of one tenth of an angstrom. In the images at the upper left of Figure 6, with little buckling and small S-Mo distances, the maxima in the image correspond to the Mo atom positions. As the buckling and/or separation is increased, image contrast changes, until the maxima correspond to the positions of the S atoms. The image corrugation, the difference between the maximum and minimum heights in each image, also increases from upper left to lower right. (This is not apparent in Figure 6 since the color contrast of each of the small images has been individually adjusted so the figure will reproduce adequately.)

It is possible to average together the unit cells within an experimental image using an autocorrelation procedure. This averaged unit cell can then be compared to theoretical simulations to determine the optimum geometry. For this case of c(2x2) S on Mo, the best fit to the experimental data gives an S-Mo distance of 0.95 angstroms and a second layer buckling of 0.22 angstroms. This is only a preliminary result. Only positive buckling (motion of the second layer Mo toward S) was considered in this set of calulations based on chemical intuition, and other work now suggests that negative buckling should also be considered. More extensive calculations are in progress. LEED I-V data has been obtained for the c(2x2) S on Mo system, and LEED structure calculations are also in progress.[14]

As can be seen by comparison of Figures 5 and 6, changes in tip chemistry and changes in surface structure can have similar results on image contrast. Experiments are currently underway to make simultaneous measurements of image contrast at multiple gap resistances. By examining both image contrast and contrast gradient at constant bias voltage, it should be possible to differentiate between tip effects and surface geometrical effects.

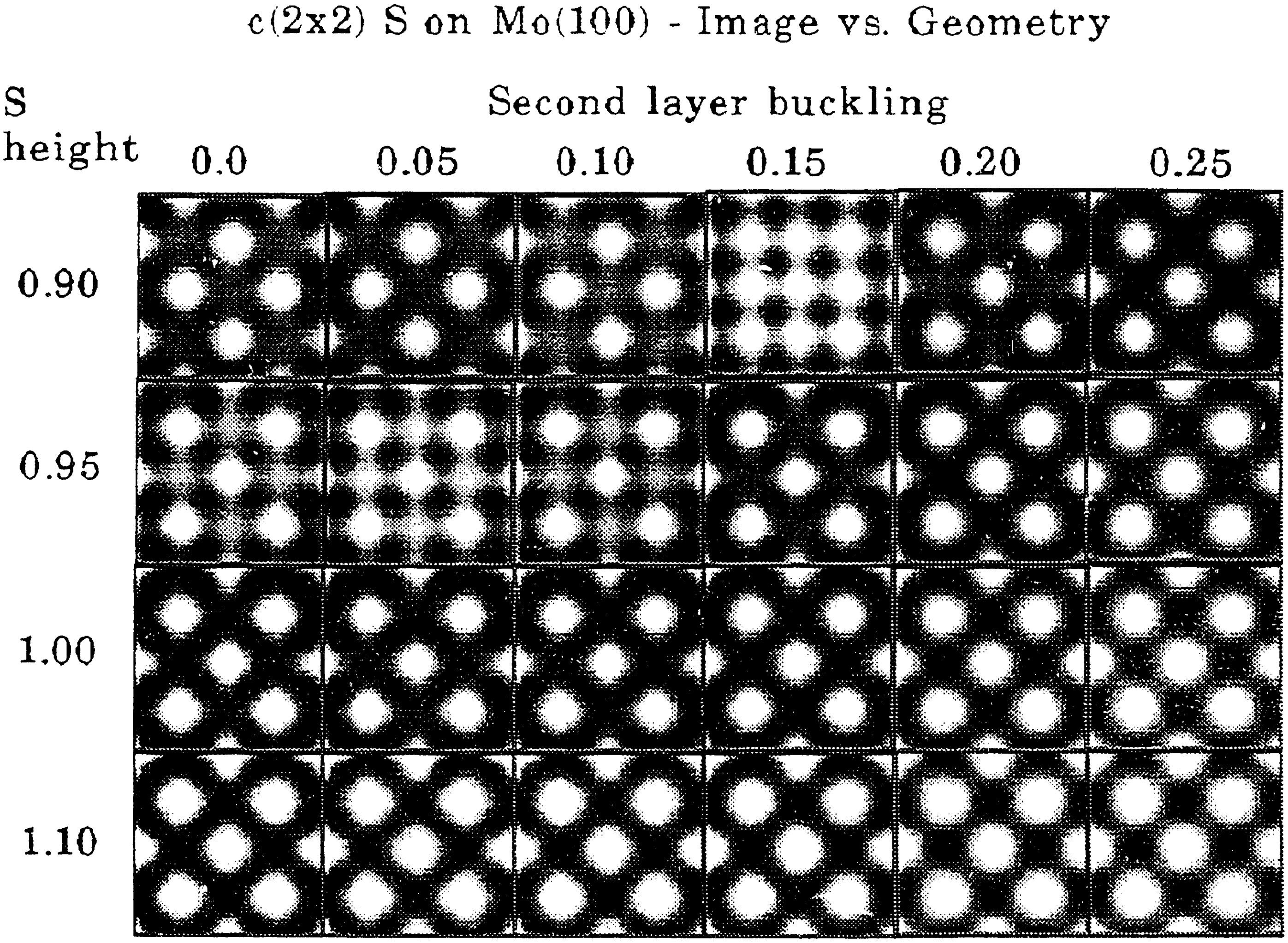
c(2x2) S on Mo(100) - Image vs. Geometry

Figure 6. Calculations of STM image contrast for a metal tip with a range of surface geometries. The vertical axis corresponds to the separation between the S-Mo planes, and the horizontal axis shows the effect of varying the height of the second layer Mo atom located beneath the S adsorption site (buckling).

6. CONCLUSIONS

The TAS scattering approach to STM theory reproduces the important features of the experimental STM images for sulfur adsorbed on Re(0001) and Mo(001). Experimentally observed variations in image contrast are shown to be consistent with changes in the nature of the tip apex atom. Since the calculations use a real-space basis, the interpretation of the theoretical results in physical terms is fairly direct. In this way we find that interference effects are significant for (2x2) S on Re(0001) with a metal tip, while surface geometry is significant for S c(2x2) on Mo(001).

The actual scattering matrix elements have been calculated using the semi-emperical Hückel approximation. Although this approximation does a good job of describing the general features of the scattering problem, it is not clear if the numerical accuracy is sufficient for determining surface structure from STM images. It should be emphasized that the TAS scattering description of STM contrast does not require the use of Hückel approximation -- more complicated methods could be used, at the cost of increased computational effort.

The usefulness of the Hückel approximation can be evaluated by comparing STM calculations for surfaces of known geometry with experimental images for a range of surfaces. We are confident that the approach described here is valid. STM calculations have been made for a number of other systems in addition to the two discussed above. Calculations are consistent with experimental STM images for the sulfur $\begin{pmatrix}3 & 1\\ 1 & 3\end{pmatrix}$ overlayer on Re(0001) with 4 S atoms per unit cell^5, for benzene adsorbed on Rh(111)^8, for graphite (0001) and for Xe on Ni(110)^{15}.

We draw two important conclusions from this work. First, the chemical identity of the STM tip atom can change image contrast. Second, changes in sub-surface atomic positions of less than one tenth of an angstrom can have a significant effect on image contrast. This complicates the interpretation of STM data, since the full surface geometry is involved, not just adsorption sites. At the same time, this sensitivity indicates that a large amount of information can be obtained through STM investigations of surface structure and bonding

7. ACKNOWLEDGMENTS

This work has been supported by the Director, Office of Energy Research, Office of Basic Energy Sciences, Materials Science Division of the US Department of Energy under contract DE-AC03-76SD00098. P. Sautet would like to acknowledge additional support from a NATO travel grant.

8. REFERENCES

1. *Ten Years of STM: Proceedings of the Sixth International Conference on Scanning Tunneling Microscopy*, Pierre Descouts and Hans Siegenthaler eds. North-Holland, 1992.

2. D. Frank Ogletree and Miquel Salmeron, "Scanning Tunneling Microscopy and the Atomic Structure of Solid Surfaces", *Progress in Solid State Chemistry* **29** 235 (90).

3. J. Tersoff and D. R. Hamann, *Physical Review Letters* **50** 1998 (83); J. Tersoff, *Physical Review* **B 39** 1052 (89).

4. N. D. Lang, *Physical Review Letters* **55** 230 (85); N. D. Lang, *Physical Review* **B 37** 10395 (88).

5. J. C. Dunphy, D. F. Ogletree, M. B. Salmeron, P. Sautet, M.-L. Bocquet and C. Joachim, "Tip Dependent Contrast in STM imaging of adsorbed sulfur layers: theory and experiment", *Ultramicroscopy* **42-44** 490 (92).

6. D. Eigler, "Atomic and molecular manipulation with the STM", *SPIE Proceedings* **1855**, paper 18 this volume (93).

7. S. Ciraci, E. Tekman, M. Gökçedag, I. P. Batra and A. Baratoff, "Adhesive energy, force and barrier height between simple metal surfaces", *Ultramicroscopy* **42-44** 163 (92); S. Ciraci, A. Baratoff and I. P. Batra, *Physical Review* **B 41** 2763 (90); S. Ciraci, A. Baratoff and I. P. Batra, *Physical Review* **B 42** 7618 (90).

8. P. Sautet and C. Joachim, *Chemical Physics Letters* **153** 511 (88); P. Sautet and C. Joachim, *Chemical Physics* **135** 99 (89); C. Joachim and P. Sautet in *Scanning Tunneling Microscopy and Related Methods*, R. J. Behm, N. Garcia and H. Rohrer eds., Kulwer, Dordrecht 1990.

9. R. Hoffman, *Journal of Chemical Physics* **39** 1397 (63) and *Reviews of Modern Physics* **60** 601 (88).

10. "The State of Surface Structural Chemistry", M. A. Van Hove, S.-W. Wang, D. F. Ogletree and G. A. Somorjai, *Advances in Quantum Chemistry* **20** 1 (1989).

11. D. Jentz, G. Held, A. Barbieri, M. A. Van Hove, G. A. Somorjai, in press.

12. "Investigation of the structures of sulfur on Mo(100) by STM", *Journal of Vacuum Science and Technology*, in press (1993).

13. P. Sautet, J. Dunphy, D. F. Ogletree, M. Salmeron, M. A. Van Hove, G. A. Somorjai, to be published.

14. M. A. Van Hove, G. A. Somorjai et al., to be published.

15. P. Sautet and C. Joachim, unpublished results.

END

DATE FILMED

11/22/93